[2.4] Chandra's First Decade of Discovery Symposium, Sep 22–25, 2009, Boston, MA

[vkashyap@cfa.harvard.edu]

Distant Suns: Solar Flares as Proxies for Stellar Flares

Vinay Kashyap, Kathy Reeves, Brad Wargelin
Smithsonian Astrophysical Observatory

SUMMARY

The solar corona has been a Rosetta stone directing our knowledge and understanding of stellar coronae. Because of its proximity, the Sun can be observed in great detail, and detailed physical models derived from such observations are often used to explain stellar phenomena.

Large stellar flares are traditionally modeled as a single coronal loop evolving hydrodynamically (see, e.g., Reale et al. 1993). However, even though this model has been successful in modeling stellar flares, it must be noted that such a picture, of a single evolving loop, has no counterpart on the Sun. Flares are observed to be complex events, generally affecting large areas of an active region and resulting in post-flare loop arcades that have a different magnetic topology compared to the pre-flare region.

Here we discuss a large flare on Ross 154 (dM3.5Ve, 2.97pc) that was seen during a Chandra observation (ObsID 2561). The flare shows (**Figure 1**) a pronounced dual-decay structure (cf. Osten & Brown 1999, Güdel et al. 2004, Reale et al. 2004), with an initial component that decays exponentially with a timescale of 400 sec, followed by another component that exponentially decays with a timescale of 13000 sec. The color-intensity diagram shows a complex, looping track during the fast decay phase and a steady softening during the long decay phase (**Figure 2**). The size of the flaring region is $L \approx 10^{10}$ cm with a density of $n_e \approx 10^{12}$ cm^{-3}, which decreases to $n_e \approx 10^{10}$ cm^{-3} during the long decay phase (Wargelin et al. 2008). *These are approximate estimates, calculated assuming a stable radiatively decaying loop.*

A new scheme has been devised recently to explain the detailed behavior of solar flares and CMEs (Reeves & Forbes 2005, Reeves et al. 2007). It relies on modeling the event as a set of cascading loops in an arcade that are sequentially energized (**Figure 3**).

Here, we explore how the solar-based model can be adapted to describe a stellar flare. Because the environments are quite different (gravity, coronal plasma density, pressure scale height, size of active region in comparison to the size of the star), and many of the required quantities of interest are unmeasured (magnetic field strength, mass of the associated CME, height of the flare, footpoint separation), the model parameters cannot be directly fit to the Chandra light curves.

We have determined that this approach holds promise. The model light curves reproduce many features of the observed data (compare **Figure 1** with **Figure 4** and **Figure 2** with **Figure 5**). Considerable exploratory work remains to be done yet to narrow down the possible parameters that may apply to the flare on Ross 154.

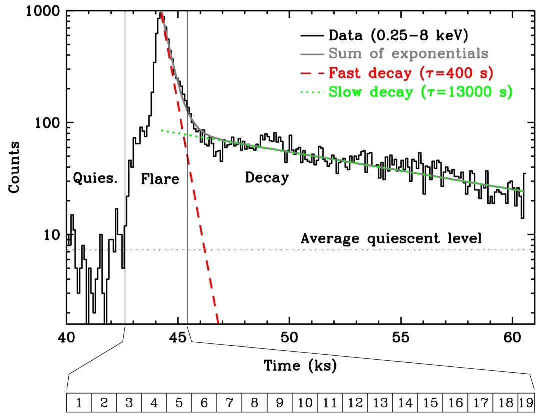

Figure 1: ACIS-S light curve of Ross 154 flare. The counts in 150 sec bins are shown over the duration of a large flare that begins at 43.8 ksec and reaches a maximum at 44.2 ksec. The peak is followed by a fast decay with a timescale $\tau = 400$ sec, and a later slower decay with $\tau = 13000$ sec. The duration of the flare rise and fast decay is expanded into a numbered set of bins below the abscissa for comparison with the color-intensity tracks in **Figure 2a**.

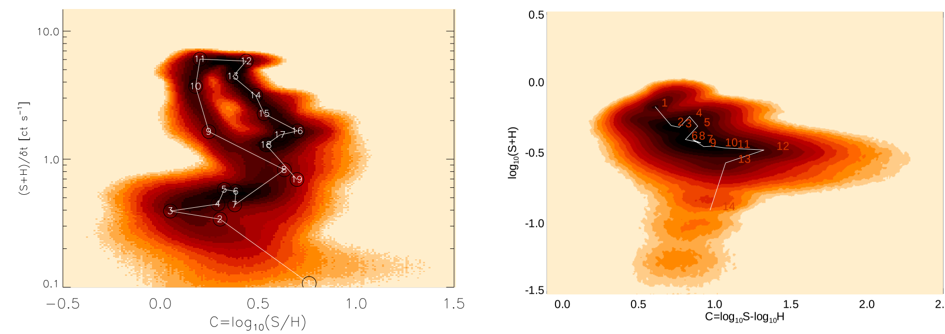

Figure 2: Color-intensity tracks for the Ross 154 flare. The color is represented by the log ratio of the counts in the soft (S = 0.25 – 1 keV) to the hard (H = 2 – 8 keV) band, and the intensity is the count rate from the two bands. The shading represents the probability that the color and intensity have a given value, with darker shades representing higher probability. The images are obtained by averaging images at various bin sizes and also cycle spun to account for the phase of the binning. *(a)* The plot on the left shows the color-intensity track for the flare rise and fast decay phase. Bin sizes ranging from 40 to 400 sec were used. Overlaid on the shaded image is the evolutionary track of the flare, labeled by the numbers corresponding to those listed at the bottom of **Figure 1**. *(b)* The plot on the right shows the color-intensity track for the long decay phase. Bin sizes range from 120 to 1100 sec, and the overlaid track is for a bin size of 1000 sec. A clear pattern in the flaring plasma evolution can be seen, with a complex looping track during the early phase, followed by a slow and steady decline during the later phase. The plasma first rises in temperature and intensity, softens at the peak, and then starts decaying in temperature and intensity. Temperatures as high as 50 MK are reached.

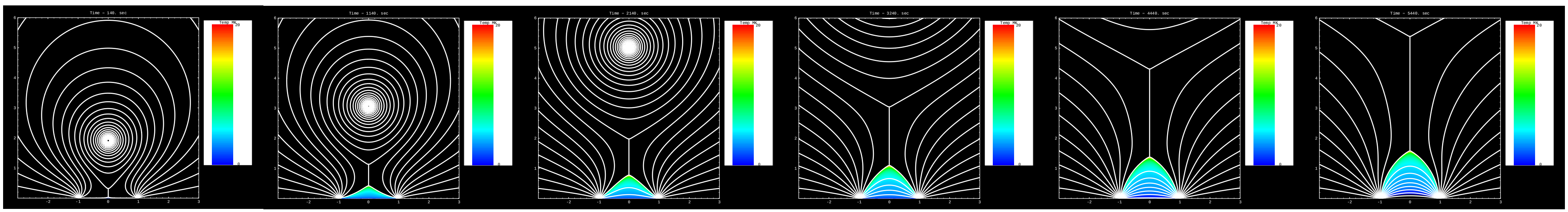

Figure 3: Evolution of an arcade after an eruption. Magnetic configurations for the loss-of-equilibrium solar eruption model are shown after the eruption and formation of the current sheet. The time elapsed after the formation of the X-point are shown at the top of each figure, and the plots are arranged in chronological sequence from left to right. The magnetic field structure is represented by the white lines. The temperatures of the plasma filling the loops is indicated by the color scale bar placed on the right. The Poynting flux swept into the current sheet determines the energy input into the reconnected flare loops. Temperatures and densities in the flare loops are calculated using the EBTEL model (Klimchuk et al, 2008). The parameters of the model are the magnetic reconnection rate represented by the Alfvénic Mach number M_A, the length scale of the footpoint separation λ_0, and the strength of the background photospheric magnetic field, B_0.

SOLAR ERUPTION AND LOOP ARCADES

The theoretical model used to generate flare light curves is devised as follows:

- A loss of equilibrium is initiated quasi-statically in a flux rope by moving the footpoints closer.
- When an eruption occurs, a current sheet forms underneath the flux rope.
- Flare loops are formed by reconnecting magnetic fields.
- The Poynting flux swept into the current sheet is assumed to fully thermalize.
- The thermal energy output is partitioned into an arcade of several hundred loops.
- The loops are currently assumed to fill sequentially at a steady rate.
- Average loop temperatures and densities are calculated using the EBTEL (Enthalpy-Baased Thermal Evolution of Loops) model (Klimchuk et al. 2008).
- Spectra are generated using PINTofALE (Kashyap & Drake 2000) for the emission measure and temperature of each loop, and are folded in through the ARF and RMF of the Ross 154 observation to obtain predicted counts.

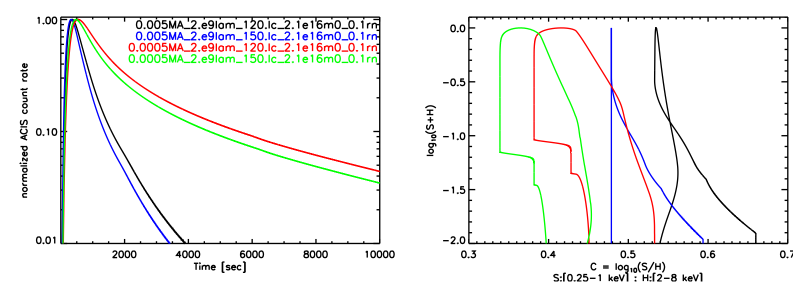

Figure 4: Model light curves and color-intensity tracks. The predicted response in ACIS-S is shown for four different models of the post-eruption arcade evolution. The models are: $\{M_A = 0.005, \lambda_0 = 2\times10^9\ \mathrm{cm}, B_0 = 120\ \mathrm{G}\}$ (black) $\{M_A = 0.005, \lambda_0 = 2\times10^9\ \mathrm{cm}, B_0 = 150\ \mathrm{G}\}$ (blue) $\{M_A = 0.0005, \lambda_0 = 2\times10^9\ \mathrm{cm}, B_0 = 120\ \mathrm{G}\}$ (red) $\{M_A = 0.0005, \lambda_0 = 2\times10^9\ \mathrm{cm}, B_0 = 150\ \mathrm{G}\}$ (green). *(a)* The figure on the left shows the light curves over the 0.3-8 keV range, and show that the typical exponential decay is modified to appear more as though there are two decay components. The early fast decay is easily replicated, and the later, longer decay can be achieved with a suitably low M_A. For instance, the $M_A = 0.0005, B_0 = 120$ G model curve can be treated as a combination of two successive exponential decays with $\tau = 800$ and 7000 sec. *(b)* The figure on the right shows the color-intensity tracks for the four models considered. A wide variety of behaviors are discernible, including those that match the observed tracks closely during the fast decay phase (**Figure 2b**). The passbands are defined in the same manner as before.

CONCLUSIONS

- We have simulated ACIS light curves from a solar eruption and arcade formation model and compared them with a large flare observed on Ross 154.
- The theoretical models duplicate many features of the observed light curves such as an extended tail in the decay, loop-like tracks in the color-intensity diagram, and large temperatures and densities.
- A further exploration of the parameter space of the model is necessary to determine "best-fit" parameters. When this is achieved, important new determinants of coronal structure, such as the height at which the flare occurs, the value of the background magnetic field, and flow velocities in the reconnection region, will become available.

REFERENCES

Güdel, M., Audard, M., Reale, F., Skinner, S.L., & Linsky, J.L., 2004, A&A, 416, 713

Kashyap, V., & Drake, J.J. 2000, Bull.Astr.Soc.India, 28, 475

Klimchuk, J.A., Patsourakos, S., & Cargill, P.J., 2008, ApJ, 682, 1351

Osten, R., & Brown, A., 1999, ApJ, 515, 746

Reale, F., Güdel, M., Peres, G., & Audard, M., 2004, A&A, 416, 733

Reale, F., Serio, S., & Peres, G., 1993, A&A, 272, 486

Reeves, K.K., Warren, H.P., & Forbes, T.G., 2007, ApJ, 668, 1210

Reeves, K.K., & Forbes, T.G., 2005, ApJ, 630, 1133

Wargelin, B.J., Kashyap, V.L., Drake, J.J., Garcia-Alvarez, D., & Ratzlaff, P.W., 2008, ApJ, 676, 610

This work was supported by CXC NASA contract NAS8–39073 (VLK, BW) and XRT NASA contract NM07AB07C (KR).